

Absolute configuration of the hydroxyfarnesylethyl group of haem A, determined by X-ray structural analysis of bovine heart cytochrome *c* oxidase using methods applicable at 2.8 Å resolution

Eiki Yamashita,^a Hiroshi Aoyama,^b Min Yao,^a Kazumasa Muramoto,^c Kyoko Shinzawa-Itoh,^c Shinya Yoshikawa^c and Tomitake Tsukihara^{a*}

^aInstitute for Protein Research, Osaka University,

3-2 Yamada-oka, Suita 565-0871, Japan,

^bRIKEN Harima Institute, Mikazuki Sayo,

Hyogo 679-5148, Japan, and ^cDepartment of

Life Science, Himeji Institute of Technology,

Kamigohri, Akoh, Hyogo 678-1297, Japan

Correspondence e-mail:

tsuki@protein.osaka-u.ac.jp

Received 7 March 2005

Accepted 22 July 2005

The absolute configuration of haem A, the prosthetic group of cytochrome *c* oxidase, was determined to be *S* by analysis of the bond angles surrounding the chiral centre of haem A after refinement with *X-PLOR* starting from respective initial structures with *R* and *S* configurations under absolute configuration constraints at 1.8 Å resolution. The same result was obtained by refinement at 1.8 Å resolution without the absolute configuration constraints. Both of these methods were applicable down to a resolution of about 2.8 Å. The constrained refinement converges more quickly than the unconstrained refinement.

1. Introduction

Because haem A, the prosthetic group of cytochrome *c* oxidase, is significantly larger, more hydrophobic and less stable than the naturally abundant protohaem, its structure was not determined until 1975 (Caughey *et al.*, 1975). The inability to crystallize this moiety despite numerous failed attempts, however, means that the absolute configuration of the chiral centre of haem A (the carbon with the OH group in the hydroxyfarnesylethyl group, as shown in Fig. 1) is still unknown. Compounding this problem is the lack of synthetic approaches that would allow determination of the absolute configuration.

Complete determination of the structure of haem A is necessary for elucidation of the reaction mechanism of cytochrome *c* oxidase, as the hydroxyl group of the chiral centre has recently been proposed to play a critical role in the enzyme's proton-pumping mechanism (Tsukihara *et al.*, 2003).

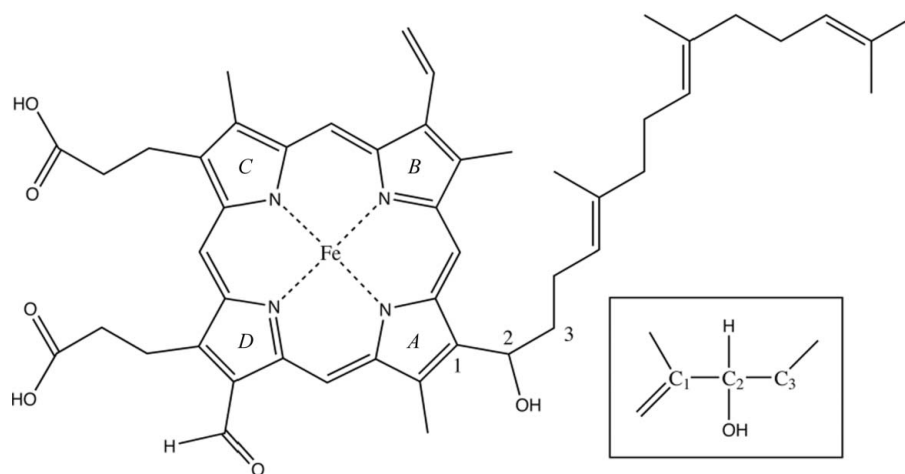


Figure 1

A schematic structural diagram of haem A. The four pyrrole rings are named A, B, C and D. A hydroxyfarnesylethyl group is attached to pyrrole ring A. The tetrahedral C atom C₂ of the hydroxyfarnesylethyl group is a chiral atom. The chemical structure around the chiral C atom is given in the box.

Table 1

Statistics of the structural refinements under absolute configuration constraints and structural statistics around the chiral atoms.

Values in parentheses are estimated standard deviations evaluated from the values for the four haems in each crystal.

	Absolute configuration of the chiral atoms of haems	
	<i>R</i>	<i>S</i>
Resolution (Å)	40.0–1.8	40.0–1.8
<i>R</i>	0.201	0.201
<i>R</i> _{free}	0.228	0.228
σ_{bond} (Å)	0.012	0.012
σ_{angle} (°)	1.8	1.8
Sums of three bond angles† (°)		
Averaged value of four haems	358.6 (1.8)	333.0 (0.9)
Averaged chiral volume‡ (Å ³)	−0.39 (0.23)	2.36 (0.05)
Resolution (Å)	10.0–2.8	10.0–2.8
<i>R</i>	0.201	0.200
<i>R</i> _{free}	0.255	0.254
σ_{bond} (Å)	0.015	0.015
σ_{angle} (°)	2.0	1.9
Sums of three bond angles† (°)		
Averaged value for four haems	345.3 (3.1)	332.6 (0.6)
Averaged chiral volume‡ (Å ³)	−1.83 (0.27)	2.40 (0.03)

† The three bond angles are C₁–C₂–C₃, C₁–C₂–OH and C₃–C₂–OH, where the atomic numbering is given in Fig. 1. The sum for each haem molecule is given in Table 2. Other statistics for the refinements have been given in previous papers (Tsukihara *et al.*, 1995, 1996, 2003; Yoshikawa *et al.*, 1998). ‡ The chiral volume of a C₂ atom is estimated by the equation $V = (R_O - R_{C2})[(R_{C1} - R_{C2}) \times (R_{C3} - R_{C2})]$, where R_X is the position vector of atom *X*. The atomic parameters for the *S* configuration are almost identical to those of PDB entries 1v54 (1.8 Å resolution) and 1occ (2.8 Å resolution).

The absolute configuration of the chiral centre can be determined using two different procedures of crystallographic refinement. These methods refine the structure with and without constraints imposed by an assumed absolute configuration of the target atom. In the present study, the absolute configuration of haem A was uniquely determined by both methods at 1.8 Å resolution and the applicability of these methods was inspected at 2.8 and 2.9 Å.

2. Methods

X-ray crystallographic analyses of oxidized, CO-bound and azide-bound cytochrome *c* oxidase from bovine heart have been reported in previous papers (Tsukihara *et al.*, 1995, 1996, 2003; Yoshikawa *et al.*, 1998). Structural refinements were performed using the program *X-PLOR* (Brünger *et al.*, 1987) under a non-crystallographic symmetry (NCS) restraint. In the *X-PLOR* refinement algorithm, the energy parameters given by Engh & Huber (1991) were applied to restrain excessive conformational changes from the standard structures, except for the S^δ–C^ε bond length of the Met residue, which was restrained using the results of Odoko *et al.* (2001). The X-ray diffraction experiments for the 2.8 Å analyses of the oxidized and CO-bound forms and the 2.9 Å analysis of the azide-bound form were carried out at 300 K (Tsukihara *et al.*, 1995), whereas high-resolution X-ray analysis of the enzyme at 1.8 Å resolution was performed at 100 K (Tsukihara *et al.*, 2003). The electron-density map of each crystal on which the structural model was superposed was calculated with the observed

structure amplitudes and the phases at the highest resolution of each crystal. The phases were obtained by extending from the initial phases determined by the molecular-replacement method at 5.0 Å using the density-modification method (Wang, 1985) coupled with NCS averaging (Buehner *et al.*, 1974; Argos & Rossmann, 1976).

Initial structural models containing a hydroxyfarnesyethyl group in either the *S* or *R* configuration were independently refined both with and without the constraints set by the initial absolute configuration of the C₂ atom (Fig. 1). The *X-PLOR* refinement has two independent functions: the first is to reduce the discrepancy between the observed and the calculated structure factors and the second is to approximate the target structure to fit with the assumed ideal structure. Thus, if an incorrect structure is assumed, the *X-PLOR* refinement produces a structure that is significantly different from the real one. When a structural refinement is performed under the constraints imposed by the mirror image of the correct configuration of a chiral centre, the structure-factor refinement tends to approximate the absolute configuration towards the correct one; on the other hand, the structural restraint maintains the incorrect mirror-image configuration even after many rounds of refinement. In consequence, a refinement procedure under the constraints for the incorrect configuration produces a flattened configuration for the chiral centre that comprises a mixture of the correct configuration and its mirror image. A chiral volume is defined by three bond vectors from a chiral atom. Since the absolute value and sign of the chiral volume represent flatness and absolute configuration, respectively, the chiral volume of each refined structure was estimated and given in Table 1.

Each round of *X-PLOR* refinement consisted of simulated-annealing refinement and subsequent positional and *B*-factor refinements. Firstly, an initial structure with an assumed absolute configuration was refined by *X-PLOR* under the constraints set by the idealized structure around the C₂ atom to eliminate the bias of the structure used for model building of the initial structure. After the structural change had converged during several rounds of *X-PLOR* refinement both with and without the absolute configuration constraints, the structural soundness of the asymmetric C atom was determined by inspecting its surrounding bond angles. The three bond angles around an asymmetric C atom in a regular tetrahedral configuration should sum to 328.5°. However, the chiral centre of haem A, which has a H atom as one of the four functional groups surrounding the chiral C atom, should have a tetrahedral configuration that is slightly flatter than normal. Analysis of 13 X-ray structures that had *R* factors less than 0.05 (El-Ferally *et al.*, 1983; Chattopadhyay *et al.*, 2001; Chen & Wu, 1999; Kohl *et al.*, 1985; Ober *et al.*, 1987; Mossa *et al.*, 1990; Ortega *et al.*, 1991; Stewart *et al.*, 1997; Banwell *et al.*, 1992; Shi *et al.*, 1997; Fahmy *et al.*, 2003; Yang & Chen, 2000) and were similar to the structure of the chiral centre of haem A deposited in the Cambridge Structural Data Base (Allen & Kennard, 1993) (Fig. 1; *i.e.* =C–HC(OH)–C–, providing that the three C atoms were not part of any ring structures) have an average value of 332.6° with an estimated standard

deviation (e.s.d.) of 3.3° for the sum of the three bond angles around the asymmetric C_2 C atom (Fig. 1; *i.e.* $C_1-C_2-C_3$, C_1-C_2-O and $O-C_2-C_3$). This averaged value was used as a reference for the present analysis.

3. Results and discussion

Fig. 2 shows the structures around C_2 with S and R configurations and the 1.8 \AA electron-density map for haem a , one of two haem A moieties within the cytochrome c oxidase enzyme. This enzyme contains two haem A molecules that serve as redox centres: one in a six-coordinated low-spin state (haem a) and the other in a five-coordinated high-spin state (haem a_3). Two analyses were performed on haem A, assuming either an S or R configuration for the chiral centre. It can clearly be seen that the atomic model for the S enantiomer fits significantly better to the electron-density map than its R counterpart (Fig. 2). This was also found to be the case for haem a_3 (data not shown). Typically, an electron-density map with a resolution as high as 1.8 \AA , as is the case here, is sufficient to determine the absolute configuration; the quality of the fit, however, cannot be evaluated quantitatively or statistically. On the other hand, the bond angles of the functional groups surrounding the chiral centre provide a quantitative measure of the strain of the fit of a particular absolute configuration. The sum of the three bond angles of the chiral centres in the 1.8 \AA X-ray structure, refined based upon the absolute configuration constraints for the S enantiomer (Table 1), was 333.7° with an e.s.d. of 1.2° ; this value is consistent with that of reference structures (332.6° with an e.s.d. of 3.3°). In contrast, when the R enantiomer was used as the model, the refinement yielded a significantly larger value, 358.6° with an e.s.d. of 1.8° , than that of the reference structure. Thus, this bond-angle analysis provided a quantitative measure of the reliability of the fit and significantly strengthened the absolute configuration determined based on the electron-density map.

An alternative X -PLOR refinement was performed without the absolute configuration constraints. The refinement at 1.8 \AA converged any haem molecule to the S configuration, regardless of whether the initial model contained an R or S enantiomer (Table 2). The refinement starting from the R enantiomer without the absolute configuration constraints, however, required more iterations than the refinement with the absolute configuration constraints before the structural refinement converged.

At 2.8 \AA resolution, it is impossible to determine the absolute configuration by a simple fit of the electron-density map; both configurations fit the map equally well (Fig. 3). The $(F_o - F_c)$ Fourier map at 1.8 \AA resolution for the R configurations exhibited significantly higher residual electron density around the chiral atom than that for S configuration, while it was impossible to distinguish the two absolute configurations by comparing 2.8 \AA $(F_o - F_c)$ Fourier maps of both configurations. The bond-angle analysis of the 2.8 \AA X -PLOR refinement with the absolute configuration restraints of the oxidized form, however, clearly identifies the absolute configuration as S (Table 1). For the fit with the S enantiomer,

Table 2

The sums of three bond angles of haem molecules in four different crystals refined both with and without absolute configuration constraints from the two different structures in respective R and S configurations.

The sum of three bond angles of $C_1-C_2-C_3$, C_1-C_2-OH and C_3-C_2-OH for each haem molecule is given in degrees. Letters S and R in parentheses represent the absolute configuration after the structural refinement. The absolute configuration of each haem molecule can be determined by comparing two sums of three bond angles for respective different initial structures in R and S configurations. The absolute configuration of haem molecules was uniquely determined as S in every case except for the haems a of CO-bound and azide-bound forms denoted by *.

	Molecule A		Molecule B	
	Haem a	Haem a_3	Haem a	Haem a_3
Oxidized (1.8 \AA)				
Constrained				
Initial structure R	359.4 (R)	360.0 (R)	355.5 (R)	359.6 (R)
Initial structure S	334.0 (S)	331.9 (S)	333.8 (S)	332.2 (S)
Non-constrained				
Initial structure R	335.5 (S)	333.3 (S)	334.7 (S)	333.6 (S)
Initial structure S	335.4 (S)	332.4 (S)	334.2 (S)	332.4 (S)
Oxidized (2.8 \AA)				
Constrained				
Initial structure R	342.4 (R)	347.9 (R)	342.1 (R)	348.9 (R)
Initial structure S	331.6 (S)	332.8 (S)	332.9 (S)	333.2 (S)
Non-constrained				
Initial structure R	330.0 (S)	332.9 (S)	333.6 (S)	332.4 (S)
Initial structure S	330.1 (S)	332.8 (S)	333.5 (S)	333.2 (S)
CO (2.8 \AA)				
Constrained				
Initial structure R	333.7 (R)*	345.0 (R)	330.2 (R)*	346.0 (R)
Initial structure S	331.0 (S)*	331.1 (S)	333.9 (S)*	330.1 (S)
Non-constrained				
Initial structure R	331.9 (R)*	329.4 (S)	327.4 (R)*	329.0 (S)
Initial structure S	329.4 (S)*	331.5 (S)	332.1 (S)*	330.4 (S)
Azide (2.9 \AA)				
Constrained				
Initial structure R	327.1 (R)*	342.7 (R)	327.3 (R)*	346.3 (R)
Initial structure S	326.1 (S)*	326.0 (S)	329.2 (S)*	324.6 (S)
Non-constrained				
Initial structure R	324.6 (R)*	326.4 (S)	325.2 (R)*	324.1 (S)
Initial structure S	324.7 (S)*	325.1 (S)	328.9 (S)*	324.4 (S)

the averaged sum of the three bond angles from the four haems was 332.6° with an e.s.d. of 1.2° . As with the refinement performed at 1.8 \AA , this value is similar to that of the reference structure. The refinement performed using the R enantiomer at 2.8 \AA resolution resulted in a flattened tetrahedral configuration, with the sum of the three bond angles averaging 345.3° with an e.s.d. of 3.1° . The structure-factor refinement tended to approximate the structure towards the S configuration; the sum of the three bond angles for the R configuration is significantly larger than that of the reference tetrahedral structure (332.5°). The value of 345.3° , however, is smaller than the 358.6° obtained from the 1.8 \AA analysis, because the refinement at 2.8 \AA resolution has fewer structure-factor terms relative to the terms of bond-angle restraints than does the 1.8 \AA analysis.

An alternative X -PLOR refinement of the oxidized form was performed without any absolute configuration constraint at 2.8 \AA . The refined 2.8 \AA structure was shown to contain haem molecules in the S configuration, regardless of whether the initial model contained an R or S enantiomer. Consequently, both procedures equivalently resulted in the correct structure, as they did at 1.8 \AA .

Both procedures were applied to the CO-bound form at 2.8 Å and the azide-bound form at 2.9 Å. These results are

listed in Table 2. *X-PLOR* refinement with the *S* configuration constraints for the CO-bound form resulted in a reasonable

range from 330.1 to 333.9° for the sum of the three bond angles for the four haems, whereas *X-PLOR* refinement with the *R* configuration constraints resulted in a flattened structure for the two structures of haem *a*₃ but not for the two structures of haem *a*. Two haem *a* molecules exhibited *R* configuration in the normal range of three bond angles. Consequently, the absolute configurations of the two structures of haem *a*₃ were determined uniquely to be *S* configuration, but the refinement under the absolute configuration constraints did not determine an absolute configuration for the two structures of haem *a*. The soundness of the refined structure was not uniform for the whole molecule. Since the two structures of haem *a* molecules were not refined as well as those of haem *a*₃, the absolute configurations of the two haem *a* structures could not be determined. The same results were obtained by the *X-PLOR* refinement without the absolute configuration constraints; that is, the structures of two haem *a* molecules whose initial structures were in *R* configuration were not converted to *S* configuration by the refinement.

The absolute configurations of the two structures of haem *a*₃ were uniquely determined by *X-PLOR* refinements both with and without the absolute configuration constraints for the azide-bound form at 2.9 Å resolution, but those of the two haem *a* structures were left undetermined as those for CO-bound form. Absolute configurations of all the haem molecules of the oxidized form were uniquely determined as *S* configuration at 2.8 Å resolution, whereas those of the CO-bound and the azide-bound forms were determined in part. Thus, the critical resolution to determine the absolute configuration of a prosthetic group is about 2.8 Å.

4. Conclusion

The resolution of an X-ray structure of a protein is determined primarily by the quality of the protein crystals, which is often impossible to improve enough to provide sufficient resolution to determine the absolute configuration of prosthetic groups by model fitting into an electron-density map. Here, we propose an effective procedure to determine the absolute configuration of a

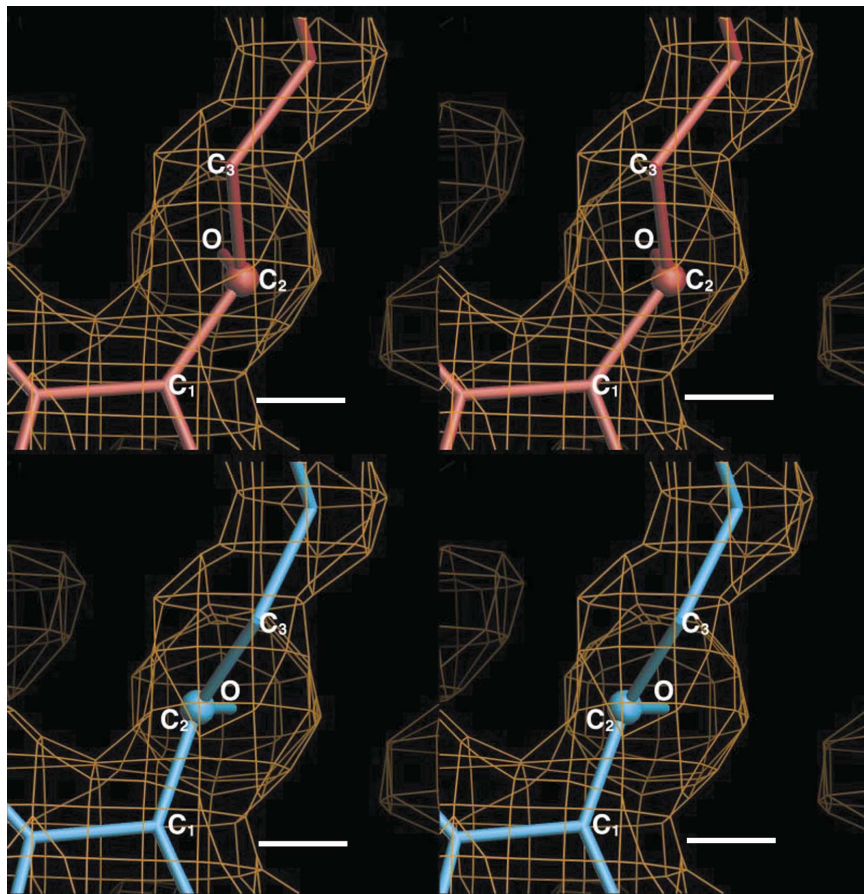


Figure 2
Refined 1.8 Å structures are superimposed upon the 1.8 Å electron-density map calculated with the observed structure amplitudes and the phases determined using the molecular-replacement method followed by density modification. Atomic names are the same as those in Fig. 1. Structures with *S* and *R* configurations are depicted by stereoscopic drawings in red (top) and light blue (bottom), respectively. The structure with the *S* configuration fits better to the electron-density map than that with the *R* configuration. The bar in each drawing is 1 Å in length.

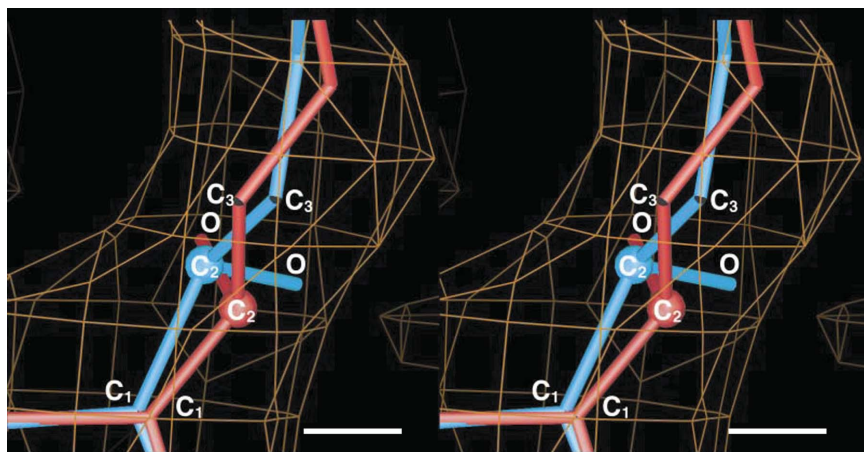


Figure 3
Refined 2.8 Å structures superimposed upon the 2.8 Å electron-density map are shown as a stereoscopic pair. The electron-density map was calculated as a 1.8 Å map. The red and light blue models are structures in *S* and *R* configurations, respectively. Both models are indistinguishable from each other with respect to their compatibility with the 2.8 Å electron-density map. The bar is 1 Å in length.

prosthetic group. Assuming the respective *S* and *R* configurations, both structures are refined independently with the constraints set by the assumed absolute configuration. When, after refinement for one of the absolute configurations, the sum of three of the bond angles of the asymmetric atom is about 332.5° , whereas after refinement for the alternative absolute configurations the sum of the bond angles converges to a significantly larger value than 332.5° , the absolute configuration is uniquely determined to be the former configuration. On the other hand, when the sums of the three bond angles obtained by the respective refinements assuming *S* or *R* configurations are not significantly different from each other, the absolute configuration is not determined. Therefore, we can assess the validity of the present method by applying it to a target structural analysis. The critical resolution to apply the method to determine the absolute configuration of haem A was about 2.8 \AA . Although the alternative procedure without the absolute configuration constraints is also applicable, it converges more slowly than the refinement with the absolute configuration constraints.

This work was supported in part by Grants-in-Aid for the 'Research for the Future' Program (JSPS-RFTF96L00503 to TT) from the Japan Society for the Promotion of Science, a research grant from the Japan Biological Informatics Consortium entrusted from the New Energy and Industrial Technology Organization (to TT), Grants-in-Aid for the 21st Century Center of Excellence Program from the Ministry of Education, Culture, Sports, Science and Technology, Japan (to TT and SY) and Grants-in-Aids for Scientific Research in Priority Areas (10188101 and 10179101 to TT and 08249106 to SY) from the Ministry of Education and Culture of Japan.

References

- Allen, F. H. & Kennard, O. (1993). *Chem. Des. Autom. News*, **8**, 31–37.
- Argos, P. & Rossmann, M. G. (1976). *Acta Cryst.* **B32**, 2975–2979.
- Banwell, M. G., Lambert, J. N., Mackay, M. F. & Greenwood, R. J. (1992). *Chem. Commun.*, pp. 974–975.
- Brünger, A., Kuriyan, J. & Karplus, M. (1987). *Science*, **235**, 458–460.
- Buehner, M., Ford, G. C., Moras, D., Olsen, K. & Rossmann, M. G. (1974). *J. Mol. Biol.* **82**, 563–585.
- Caughey, W. S., Smythe, G. A., O'Keefe, D. H., Maskasky, J. E. & Smith, M. L. (1975). *J. Biol. Chem.* **250**, 7602–7622.
- Chattopadhyay, S. K., Sharon, A., Yadav, U., Srivastava, S., Mehta, V. K. & Maulik, P. R. (2001). *Acta Cryst.* **E57**, o1158–o1160.
- Chen, K. & Wu, Y. (1999). *Tetrahedron*, **55**, 1353–1366.
- El-Ferally, F. S., Benigni, D. A. & McPhail, A. T. (1983). *J. Chem. Soc. Perkin Trans.* **1**, 355–364.
- Engl, R. A. & Huber, R. (1991). *Acta Cryst.* **A47**, 392–400.
- Fahmy, H., Zjawiony, J. K., Khalifa, S. & Fronczek, F. R. (2003). *Acta Cryst.* **C59**, o85–o87.
- Kohl, W., Witte, B., Kunze, B., Wray, V., Schomburg, D., Reichenbach, H. & Hofle, G. (1985). *Liebigs Ann. Chem.*, pp. 2088–2097.
- Mossa, J. S., Mohammed, A., Al-Yahya, M. A., Hifnawy, M. S., Shehata, A. A., El-Ferally, F. S., Hufford, C. D., McPhail, D. R. & McPhail, A. T. (1990). *Phytochemistry*, **29**, 1595–1599.
- Ober, A. G., Fronczek, F. R. & Fischer, N. H. (1987). *J. Nat. Prod.* **50**, 604–611.
- Odoko, M., Yao, M., Yamashita, E., Nakashima, R., Hirata, K., Aoyama, H., Muramoto, K., Shinzawa-Itoh, K., Yoshikawa, S. & Tsukihara, T. (2001). *J. Appl. Cryst.* **34**, 80–81.
- Ortega, A., Cardenas, J., Toscano, A., Maldonado, E., Aumelas, A. & Van Calsteren, M. R. (1991). *Phytochemistry*, **30**, 3357–3360.
- Shi, Q., Verdier-Pinard, P., Brossi, A., Hamel, E., McPhail, A. T. & Lee, K. (1997). *J. Med. Chem.* **40**, 961–966.
- Stewart, M., Blunt, J. W., Munro, M. H. G., Robinson, W. T. & Hannah, D. J. (1997). *Tetrahedron Lett.* **38**, 4889–4890.
- Tsukihara, T., Aoyama, H., Yamashita, E., Tomizaki, T., Yamaguchi, H., Shinzawa-Itoh, K., Nakashima, R., Yaono, R. & Yoshikawa, S. (1995). *Science*, **269**, 1017–1188.
- Tsukihara, T., Aoyama, H., Yamashita, E., Tomizaki, T., Yamaguchi, H., Shinzawa-Itoh, K., Nakashima, R., Yaono, R. & Yoshikawa, S. (1996). *Science*, **272**, 1136–1144.
- Tsukihara, T., Shimokata, K., Katayama, Y., Shimada, H., Muramoto, K., Aoyama, H., Mochizuki, M., Shinzawa-Itoh, K., Yamashita, E., Yao, M., Ishimura, Y. & Yoshikawa, S. (2003). *Proc. Natl Acad. Sci. USA*, **100**, 15303–15309.
- Wang, B.-C. (1985). *Methods Enzymol.* **115**, 90–112.
- Yang, K. & Chen, K. (2000). *Org. Lett.* **2**, 729–731.
- Yoshikawa, S., Shinzawa-Itoh, K., Nakashima, R., Yaono, R., Yamashita, E., Inoue, N., Yao, M., Fei, M. J., Peters-Libeu, C., Mizushima, T., Yamaguchi, H., Tomizaki, T. & Tsukihara, T. (1998). *Science*, **280**, 1723–1729.